ACS APPLIED MATERIALS & INTERFACES

RESEARCH ARTICLE

www.acsami.org

Preparation of Protein- and Cell-Resistant Surfaces by Hyperthermal Hydrogen Induced Cross-Linking of Poly(ethylene oxide)

Colin V. Bonduelle,[†] Woon M. Lau,[†,‡] and Elizabeth R. Gillies*[,†,§]

[†]Department of Chemistry, The University of Western Ontario, 1151 Richmond Street, London, Canada N6A 5B7

[‡]Surface Science Western, The University of Western Ontario, London, Ontario, Canada N6A 5B7

[§]Department of Chemical and Biochemical Engineering, The University of Western Ontario, 1151 Richmond Street, London, Canada N6A 5B9

Supporting Information

ABSTRACT: The functionalization of surfaces with poly(ethylene oxide) (PEO) is an effective means of imparting resistance to the adsorption of proteins and the attachment and growth of cells, properties that are critical for many biomedical applications. In this work, a new hyperthermal hydrogen induced cross-linking (HHIC) method was explored as a simple one-step approach for attaching PEO to surfaces through the selective cleavage of C−H bonds and subsequent cross-linking of the resulting carbon radicals. In order to study the effects of the process on the polymer, PEO-coated silicon wafers were prepared and the effects of different treatment times were investigated. Subsequently, using an optimized treatment time and a modified butyl polymer with increased affinity for PEO, the technique was applied to butyl rubber surfaces. All of the treated surfaces exhibited significantly reduced protein adsorption and cell growth relative to control surfaces and compared favorably with surfaces that were functionalized with PEO using conventional chemical methods. Thus HHIC is a simple and effective means of attaching PEO to non-functional polymer surfaces.

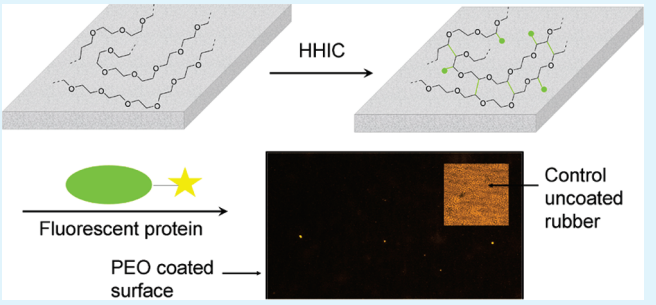

KEYWORDS: PEO grafting, protein resistance, non-fouling properties, collision-induced cross-linking, butyl rubber, coatings

INTRODUCTION

Materials that resist the adsorption of proteins as well as the adhesion and growth of cells are critical in many applications ranging from protein purification to medical devices.[1,2] Thus far, the functionalization of surfaces with poly(ethylene oxide) (PEO) has proven to be one of the most effective means of achieving the desired nonfouling properties.[3,4] PEO is commonly used in the chemical industry, in biochemistry and in biotechnology because of its biocompatibility.[3] It is proposed that surface-grafted PEO chains prevent protein adsorption primarily by steric repulsion,[5,6] whereas electrostatic repulsion is also of importance in the low-molecular-weight cases.[7] The protein resistance has also been attributed to the high water content of PEO,[8,9] to its large excluded volume' and to its prevention of access to adsorption sites on the underlying surface.[11]

Thus far, several different approaches have been explored for the functionalization of surfaces with PEO. Many examples have involved the covalent attachment of PEO to reactive surfaces by (1) silanation using either a silane functionalized PEO or a silane precursor bearing another functionality that can couple with an end-functionalized PEO,[7,12−15] (2) the reaction of amine functionalized surfaces with PEO derivatives,[16,17] and (3) the reaction of electrophilic surface groups with nucleophilic PEO derivatives.[15,18,19] In the study of various PEO-functionalized surfaces, it has been found that protein adsorption generally decreased with increasing length of the PEO as well as with increasing grafting density.[11,13,14,17,20−23] Noncovalent methods including physisorption[24,25] and chemisorption[7,20−23,26−28] have also been investigated to introduce PEO. For example, after initiator adsorption followed by surface-initiated polymerization of oligo(ethylene glycol) methacrylate the lowest known protein adsorption has been achieved.[29,30] However, these methods do not provide a strong attachment of the polymer to the surface, which may affect the stabilities of the resulting surfaces. Overall, the above approaches have been successful in allowing a high degree of control over the chemical structures of the polymers on the surface. Nevertheless, the successful grafting or adsorption of PEO is often challenging because of the excluded-volume effect[31,32] which limits the surface density of the polymer chains. Moreover, these approaches require specific functional groups on the surface to covalently or non-covalently graft the PEO. Consequently, each approach is substrate specific. Finally, the solution phase nature of the processes and the requirements for excess reagents make these methods costly for industrial scale up.

Received: February 25, 2011
Accepted: April 15, 2011
Published: April 15, 2011

The use of a physical treatment is an alternative approach for the formation of PEO functionalized surfaces. With this approach, by coating a surface with PEO and subsequently performing a plasma-induced cross-linking[33−35] or an electron beam-induced cross-linking,[36] non-fouling properties were achieved. Plasma processes have also been used to induce polymerization processes via radical formation to provide a polymeric layer having a 'PEO character' with non-fouling properties. For that purpose, tetraglyme,[37,38] triglyme,[38] or diglyme[38−41] were used, but other oligomers of PEO containing vinyl/allyl end functionalities were also reported.[42,43] In the best of the cases, the plasma approach has resulted in thin films composed mainly of ethylene oxide units, like those in PEO, along with a certain degree of cross-linking.[41,43] Although the use of physical treatments has the advantage that is not substrate specific and is more cost-effective than traditional wet chemistry, the hot electrons, ions, radicals and other excited or energetic species can lead to partial surface destruction or to the formation of undesirable surface chemical functionalities. For example, side reactions resulting in other moieties such as esters, carbonyls, carboxyls, and hydrocarbon groups are often observed,[41,42] as well as a decrease in the oxygen content of the layer.[39,41,44]

Recently, a new dry-process approach to synthesize molecular layers with tailor-made functionalities was developed by using the concept of collision kinematics. This method is fundamentally different from the conventional use of chemistry or plasma as it involves an unusual mix of physical and chemical processes including charge exchange, projectile penetration, kinematics, collision-induced dissociation, inelastic energy transfer, chain transfer, and chain cross-linking. The first applications of this method involved the treatment of surfaces with H^+ projectiles having elevated kinetic energy[45] but the use of energetic H_2 projectiles was recently developed to avoid the build up of charge on insulating substrates such as polymers.[46] According to the hard sphere approximation, the maximum energy transfer between two colliding species is determined by the two masses with the formula $4M_1M_2/(M_1+M_2)^2$. This simple model suggests that for a projectile of H_2, in the head-on collision with H of a C−H bond, the maximum kinetic energy transfer is 89%, whereas if the target is C, the maximum kinetic energy transfer is 49%. Thus by considering bond dissociation energies and controlling the energy of the H_2 projectiles accordingly, in principle this process provides the advantage of being able to cross-link molecular films by specific C−H bond cleavage followed by radical combination, while preserving other chemical functionalities of the molecules on the surface. Indeed the first process using H^+ projectiles has even afforded selectivity for the cleavage of C−H bonds over the O−H bonds of carboxylic acids in thin films of poly(acrylic acid), selectivity that was derived from the bond strength difference between C−H and O−H. The theoretical framework has also been lifted from the oversimplified model derived from the hard sphere approximation to the results from ab initio molecular dynamics computation[45] for selective C−H cleavage with both hyperthermal H^+ and H_2. Moreover and unlike the conventional wet-chemistry synthesis of cross-linked polymeric films, this new route uses no chemical initiators, additives, nor catalysts, and only requires molecular hydrogen with a kinetic energy of a few electron volts. A practical reactor giving a high flux of such hyperthermal hydrogen for complete surface grafting in seconds has recently been developed.[46]

We report here the first application of hyperthermal H_2-induced cross-linking (HHIC) for the creation of non-fouling surfaces. It is demonstrated that this method can be used to create cross-linked PEO films in a single step without significant side reactions and that these surfaces can resist the adsorption of proteins and the adhesion of cells. The effect of the treatment time on the chemical structure of the PEO films is studied by atomic force microscopy (AFM), X-ray photoelectron spectroscopy (XPS), and contact angle analysis in order to gain insight into the mechanism, scope and limitations of the technique. In addition, the use of this approach for the preparation of the first non-fouling PEO functionalized butyl rubber surfaces is described, thus demonstrating the versatility of the HHIC process for the functionalization of non-reactive, hydrophobic polymer surfaces.

EXPERIMENTAL SECTION

Materials. Glass coverslips (1.8 mm, number 2) were purchased from Corning, USA. Silicon wafers were purchased from University Wafer (Boston, USA). Butyl rubber 402 and cured butyl rubber 08CA361 were provided by LANXESS, Inc. Sarnia, Canada. Poly(ethylene oxide) (PEO, MW = 100 000 g/mol) or poly(ethylene glycol) monomethyl ether (m-PEG, MW = 5000 g/mol), 3-isocyanatopropyltriethoxysilane (IPTS, 95%), dibutyltin dilaurate, Rhodamine B, 4′,6-diamidino-2-phenylindole (DAPI) and fibrinogen (from human plasma) were purchased from Sigma/Aldrich. C_2C_{12} cells, culture media (fetal bovine serum (FBS), Glutamax, Glucose, Penstrep), trypsin solution and phosphate buffered saline (PBS) 10× solutions were purchased from Invitrogen. All chemicals were used without further purification.

Preparation of Surfaces. Glass coverslips and silicon wafers were cleaned by immersion in H_2O_2/H_2SO_4 solution overnight. They were then rinsed with deionized distilled water and dried at 100 °C. For characterization of resistance to protein adsorption: Thin films of PEO were prepared by spin coating a solution of PEO in CH_2Cl_2 (4 mg/mL, 100 μL for 1 cm^2, 6000 rpm, 30 s) on a clean silicon wafer or on an epoxidized butyl coated silicon wafer. Thin films of butyl rubber were prepared by spin coating a solution of butyl 402 in hexane (5 mg/mL, 100 μL for 1 cm^2, 6000 rpm, 30 s) on a clean silicon wafer. Thin films of epoxidized butyl were prepared by spin coating a solution of epoxidized butyl rubber in hexane (5 mg/mL, 100 μL for 1 cm^2, 6000 rpm, 30 s) on a clean silicon wafer or on a butyl coated silicon wafer. For cell culture: A sheet of bulk cured butyl rubber 08CA361 was washed by immersion in water for 24 h and then cut and sterilized by UV light (1 h). This washed sheet of butyl rubber was also spin coated with epoxidized butyl rubber in hexane (5 mg/mL, 100 μL for 1 cm^2, 6000 rpm, 30 s) followed by PEO in CH_2Cl_2 (4 mg/mL, 100 μL for 1 cm^2, 6000 rpm, 30 s) twice. Thin films of PEO were prepared by spin coating a solution of PEO in CH_2Cl_2 (4 mg/mL, 100 μL for 1 cm^2, 6000 rpm, 30 s) on a clean silicon wafer.

Hyperthermal Hydrogen-Induced Cross-Linking. HHIC of the film was carried out in a custom designed reactor that is described in more detail in the Supporting Information. Typically, the specimen was exposed to hyperthermal molecular hydrogen with a nominal average kinetic energy of 5−10 eV with a fluence of 1×10^{15} to 1×10^{18}/cm^2. The typical fluence in this work was about 1×10^{16} to 1×10^{17}/cm^2 and the fluence was accumulated on the specimen within a few seconds.

XPS Analysis. XPS analyses were carried out with a Kratos Axis Ultra spectrometer using a monochromatic Al K(alpha) source (15 mA, 14 kV). The instrument work function was calibrated to give a binding energy (BE) of 83.96 eV for the Au $4f_{7/2}$ line for metallic gold and the spectrometer dispersion was adjusted to give a BE of 932.62 eV for the Cu $2p_{3/2}$ line of metallic copper. The Kratos charge neutralizer system was used on all specimens. Survey scan analyses were carried out with an analysis area of 300 x 700 micrometers, a pass energy of 160 eV and a 45° take-off angle. High resolution analyses were carried out with an analysis area of 300 x 700 micrometers, a pass energy of 20 eV and 45° take-off angle. Spectra have been charge corrected to the main line of the carbon

1s spectrum (adventitious carbon) set to 285.0 eV. Spectra were analysed using CasaXPS software (version 2.3.14).

Contact Angle Measurements. A contact angle goniometer (Ramé-Hart's Model 100-00) was used. Surfaces were first loaded onto the stage and drops of distilled water were placed on the specimens. The reported static angles were calculated by averaging the angles from both the left and right sides of the droplet. Advanced and receding contact angles were also evaluated. At least 10 measurements on each surface were obtained for each experimental condition.

AFM analysis. Surfaces were visualized by an atomic force microscope (XE-100 microscope from PSIA). Images were obtained by scanning a surface of 20 μm × 20 μm in a tapping mode using rectangular-shaped silicon cantilevers with a spring constant of 48 N/m. Data were then refined using the software XEI and digitally obtained scans were graphically modified by using the software Gwyddion.

Functionalization of Glass Surfaces with Silane-Functionalized PEO. PEO-grafted glass surfaces were prepared following a previously reported procedure involving the silanation of glass surfaces with (N-triethoxysilylpropyl)-*O*-monomethoxy PEG urethane in ethanol.[12]

Protein Adsorption. A solution of the previously reported Rhodamine-fibrinogen conjugate[47] in 5 mM phosphate buffer, pH 7.2 was prepared; 1 mg/mL of protein was used in the experiment comparing the PEO surfaces treated for different times, whereas 400 μg/mL of protein was used in all other experiments. The surfaces were then immersed in the protein solution. After 2 h, the nonadsorbed protein was removed by washing the surfaces with buffer and water. The fluorescence was then evaluated by using an LSM 510 multichannel point scanning confocal microscope (laser 543 nm and band pass filter of 560−600 nm). The fluorescence was evaluated by averaging 10 randomly selected regions of the surface within each sample. Linear operation of the camera was ensured, and the constant exposure time used during the image collection permitted quantitative analyses of the observed fluorescent signals. The fluorescence microscopy images were analyzed using the software Northern Eclipse Image Analysis (Empix Imaging, Mississauga, Ontario), which yielded the mean and standard deviation of the fluorescence intensity within a given image. The fluorescence intensity of a region of the surface that was not exposed to protein was measured in order to quantify the background fluorescence of the material itself and this value was subtracted from the fluorescence measured for the exposed regions. The background-corrected fluorescence intensity for each film was then used to compare the protein adsoption on each surface. For all the samples, three surfaces were prepared and measured.

Evaluation of Cell Growth. C_2C_{12} mouse fibroblast cells were cultured in growth medium composed of an optimal mix of an FBS solution (50 mL), Glutamax solution (5 mL), Glucose solution (1L) and Penstrep solution (5 mL). 1×10^4 cells were seeded on each of the prepared surfaces (1 cm^2). These cells were incubated in the growth medium described above at 37 °C (5 % CO_2). After 48 h, the growth medium was aspirated and the surfaces were washed 3 times with PBS (pH 7.2). The cells were then incubated for 10 minutes with a paraformaldehyde fixing solution (400 mg in 10 mL of PBS 10×, pH 7.2) and then washed 3 times with PBS (pH 7.2). After fixation, the surfaces were immersed in cold acetone (3 min) and in PBS buffer (10 min) for permeation. Finally, the surfaces were immersed in a DAPI solution (1 μg/mL in water) to stain the cell nuclei. The number of cells on each surface was then evaluated by fluorescence microscopy. Ten randomly selected regions were averaged for each surface. For each sample, three surfaces were prepared and measured.

RESULTS AND DISCUSSION

Coating and Cross-Linking of PEO on a Silicon Wafer. A silicon wafer was selected as an initial substrate on which to study the PEO coating and cross-linking process as it is atomically smooth, facilitating the characterization of the surface using techniques such as AFM and XPS. PEO with a molecular weight of 100 00 g/mol was used to create thin films on the wafers by spin-coating from CH_2Cl_2. The thicknesses and the roughnesses of the obtained layers were determined by AFM. Different thicknesses were readily obtained by simply tuning the PEO concentration, while the roughness remained relatively constant (Table 1). A PEO concentration of 4 mg/mL was selected to prepare the surfaces for HHIC as the normal depth of cross-linking is approximately 10−20 nm.[45]

Table 1. Thicknesses and Roughnesses of Spin-Coated PEO films As Determined by AFM Analysis

concentration of PEO in $CHCl_3$ (mg/mL)	thickness (nm)	roughness (nm)
2	8	2.1
3	12	1.9
4	19	2.9
5	26	2.3

Table 2. XPS Analyses of Cross-Linked and Non-Cross-Linked PEO-Coated Silicon Wafers before and after Washing

		composition (%)		
HHIC	wash	C	O	Si
yes	yes	73.9	26.1	
yes	no	73.3	26.7	
no	yes	21.3	33.0	45.7
no	no	74.0	26.0	

Treatment of the PEO coated silicon wafers with HHIC for 100 s was then performed. To determine whether the PEO was successfully cross-linked on the surface, a wash test and XPS analyses were performed. Prior to cross-linking, only peaks corresponding to C and O were observed in XPS analyses, confirming that these surfaces were indeed coated with PEO (Table 2). Following cross-linking there was no significant change in the C versus O composition. Washing of the noncross-linked surfaces for 2 days in water revealed a strong peak corresponding to Si in the XPS analysis, indicating that the uncross-linked polymer was washed from the surface. In contrast, when the cross-linked surfaces were washed, the XPS spectra did not change, thus indicating that the polymer could not be washed from the surface. High resolution XPS (HR-XPS) data were obtained to further probe the structure of the PEO layer. Analysis of the C 1s signal revealed an increase in the intensity of the C−C peak corresponding to the formation of carbon atoms that are not linked to oxygens as they were in the initial PEO chain, as well as a very small peak corresponding to O−C═O bond formation (Table 3). Nevertheless the PEO character of the cross-linked layer, as measured by XPS, was almost 90% after 100 s of HHIC, while the best results obtained for other physical treatment processes were around 70 - 80%, with most results being lower.[39,41,44,48] In addition, the surface roughness remained very low at approximately 2 nm (see the Supporting Information) in comparison to 5−10 nm often observed for physical treatment processes, thus demonstrating the non-ablative effect of HHIC.

Table 3. XPS Analyses of the PEO-Coated Silicon Wafers before and after HHIC for Different Times

			HR-XPS C 1s				
treatment time	C 1s	O 1s	O−C═O	C═O	C−O	Cyclic C−O	C−C
none	74.9	25.1			98.3		1.7
100 s	74.7	25.3	2.6		87.5		9.9
400 s	72.0	28.0	4.1	38.5	34.2	12.5	10.7
1000 s	73.8	26.2	6.7	30.2	24.0	13.3	25.7

Table 4. Contact Angle measurements of PEO-coated silicon wafers following HHIC for different time periods

treatment time (s)	static contact angle (deg)	advancing contact angle (deg)	receding contact angle (deg)
100	24.4 ± 1.0	27.6 ± 2.1	<10
400	35.0 ± 2.2	47.4 ± 2.9	16.9 ± 5.2
1000	52.4 ± 2.9	58.8 ± 1.8	25.8 ± 3.5

Table 5. Analyses of Cross-Linked Butyl Rubber and PEO-Coated Butyl Rubber Films by AFM (nd = not determined)

sample	film thickness (nm)	film roughness (nm)
butyl 402	22	1.8
epoxidized butyl 402	23	1.3
butyl 402 + PEO (100 KDa)	nd	nd
epoxidized butyl 402 + PEO (100 KDa)	36	5.9

The next step was to explore the effect of prolonged treatment times on the structure of the PEO layer and the resulting resistance to protein adsorption. There are a couple of reasons why this is important. Firstly, when PEO has been grafted onto surfaces at sufficiently high densities by reactions between the PEO terminus and the surface, it has been proposed to exhibit a brush-like architecture.[8,49] Some authors have suggested that the conformational mobility of the PEO chains produces an entropic penalty during chain compression if protein adsorption occurs,[5,23,50−52] and consequently PEO chain mobility on such surfaces is thought to be important for optimizing the resistance to protein adsorption. In contrast, when PEO is introduced to the surface by HHIC, cross-links can occur at multiple points along a given PEO chain, thus fixing the chains, preventing the formation of brushlike structures, and reducing the chain mobility. While it is not possible to exactly quantify the number of cross-links per polymer at a given treatment time, they presumably increase with increased surface treatment times, and it is of fundamental interest to study the effect of the degree of cross-linking on the nonfouling properties. Secondly, it was important to determine at what point extended treatment times can lead to side reactions that significantly alter the chemical structure of the PEO layer.

Two additional treatment times of 400 s and 1000 s were selected for comparison with the 100 s results. After cross-linking, each sample was analyzed by AFM. No significant changes in the layer thickness or roughness were observed (see the Supporting Information). The samples were also analyzed by XPS. The resulting spectra revealed that no changes in the C/O composition were observed, even after 1000 s of treatment (Table 3), contrary to conventional plasma grafting of PEO-like surfaces where significant changes in the C/O composition are observed.[39,41,53] However, high-resolution C 1s spectra exhibited changes with increased treatment time. These changes were explained by the appearance of additional C−C bonds, cyclic C−O bonds, C═O bonds, and O−C═O bonds. Although the cyclic C−O bonds could be expected to arise from extensive cross-linking (see the Supporting Information), the C−C, C═O, and O−C═O bonds must arise from rearrangement processes, likely attributable to side reactions of the radicals.

Contact angle measurements were also performed to further analyze the cross-linked PEO surfaces (Table 4). Although the contact angle of the un-cross-linked, spin-coated film could not be measured because of its solubility in water, following 100 s of HHIC the contact angle was 24°, very similar to that measured for surfaces with grafted PEO chains.[12] The contact angle increased up to 52° after 1000 s of treatment. The advancing and receding contact angles also increased with treatment time (Table 4). As the same C/O ratio was observed by XPS after all treatment times, a chemical reorganization had occurred without lost of oxygen. It is possible that the side reactions evidenced by XPS in the samples treated for long time periods exhibit inferior hydrogen bonding capabilities than the linear PEO, and thus lower hydrophilicity. Overall, the above results suggest that HHIC can successfully be used to form stable cross-linked PEO films, and that shorter treatment times no more than 100 s result in minimal disruption of the PEO chemical structure.

Coating and Cross-Linking of PEO on Butyl Rubber. One of the challenges in using the PEO grafting approach is the functionalization of substrates lacking reactive groups. In contrast, using HHIC it should be possible to cross-link thin films on a wide variety of nonreactive substrates. Butyl rubber is a polymer of emerging interest for biomaterials applications. It has been proposed as an ideal material for breast implants because of its impermeability and nonbiodegradability.[54,55] Additionally, copolymers of polyisobutylene with polystyrene are currently being used in vascular stents.[56] However, it has been argued that it will be necessary to reduce the adsorption of proteins to its surface in order to exploit its full potential.[55] As a polymer containing only C−H bonds from the polyisobutylene with a small fraction (approximately 2%) of C═C bonds from isoprene, it is an ideal substrate for functionalization by HHIC.

To aid in the characterization of the functionalization process and analysis of the protein adsorption, we obtained a flat butyl rubber surface by spin-coating butyl 402 on a silicon wafer. This surface was cross-linked by HHIC. AFM analysis was used to measure the film thickness and roughness, which were determined to be 22 and 1.8 nm, respectively (Table 5, Figure 1a). The next step was to spin-coat PEO on this butyl surface. Unfortunately, because of the incompatibility between PEO and butyl, the resulting film was highly inhomogeneous with large drops of PEO observed on the surface (Figure 1b). Other work in our laboratories involved the preparation of an epoxidized butyl by reacting the 2% isoprene units in butyl with m-chloroperoxybenzoic acid (Figure 2).[47] This polymer was spin-coated on a silicon wafer and cross-linked for 100 s to provide a film thickness of 23 nm and a roughness of 1.3 nm (Figure 1c) as measured by AFM. High resolution C 1s spectra confirmed the presence of the epoxide functionality, indicating that it survived the HHIC (see the Supporting Information). Next, the spin coating of PEO on this modified butyl surface was attempted. The PEO layers

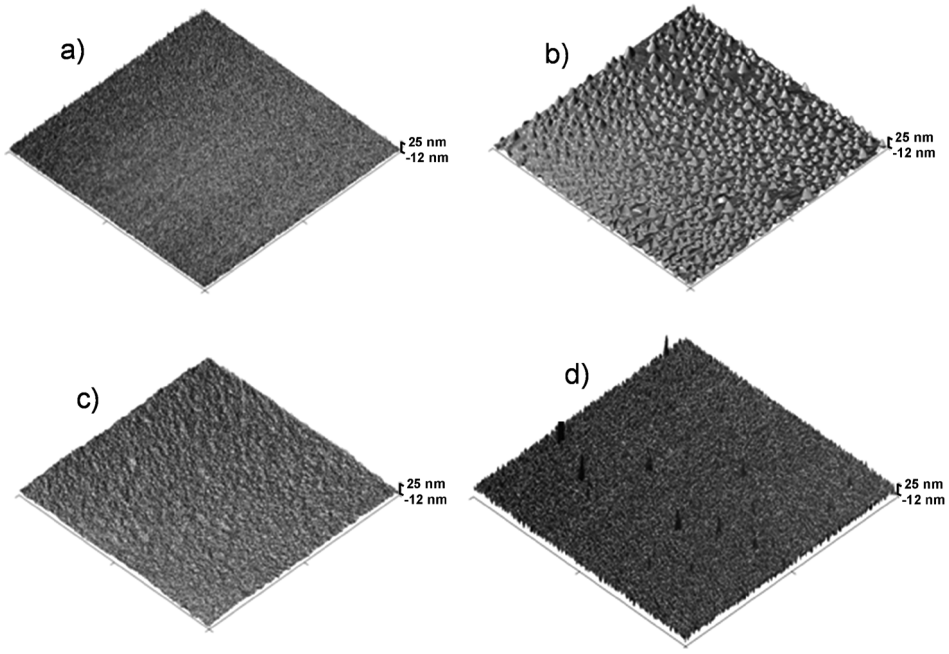

Figure 1. AFM images (topography) of films: (a) cross-linked butyl rubber; (b) PEO (100 KDa) on cross-linked butyl rubber; (c) cross-linked epoxidized butyl rubber; (d) PEO (100 KDa) on cross-linked epoxidized butyl rubber. Each image represents a 20 × 20 μm area.

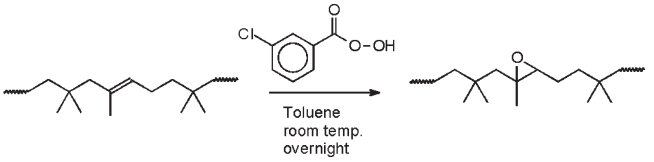

Figure 2. Epoxidation of the butyl rubber.

on this surface were much more uniform and a combined film thickness of 36 nm and a roughness of 5.9 nm were measured for the butyl and PEO layers combined (Figure 1d). This result was reproducible. The PEO was subsequently cross-linked for 100 s to provide a stable film that resisted washing.

It is noteworthy that the epoxide functionality on the butyl has been found to be remarkably unreactive in solution, except under strongly basic or strongly acidic conditions. Given the increased difficulties of performing reactions on surfaces, the ring-opening of the epoxide by the hydroxyl of the PEO under the conditions of the spin-coating is an extremely unlikely cause of the increased film uniformity. In addition, the thin film of epoxidized butyl was found to have a contact angle of 88°, very close to the 91° obtained for the thin film of butyl, indicating that the hydrophilicities of the two surfaces are not very different. Perhaps it is the increased oxophilicity that results from the incorporation of even small percentages of oxygen into the butyl that enhances the compatibility between the two polymers. This oxophile effect was previously observed by Mondragon et al. when epoxy resins were mixed with polybutadiene copolymers.[57] An introduction of 4.8% of epoxidised polybutadiene units in the overall mixture was enough to achieve a nanostructuring of the final polymer blend. In our case, the epoxidized butyl or other hydrophobic polymers that are oxidized to small degrees may provide a general strategy for increasing the compatibility of hydrophobic polymer surfaces with PEO and other hydrophilic polymers, thus allowing them to be effectively spin-coated. Studies are currently

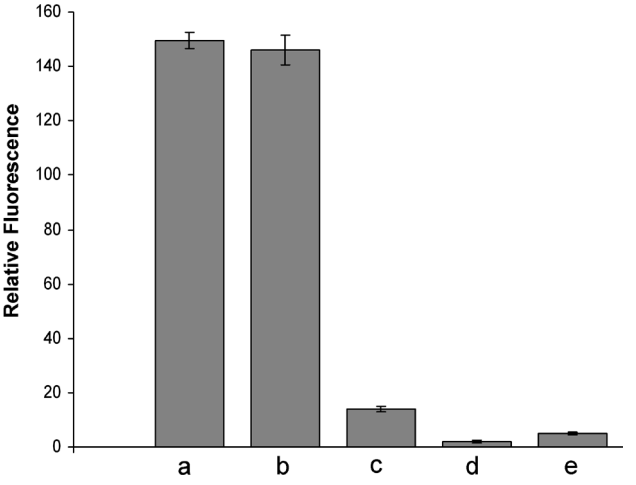

Figure 3. Relative fluorescence obtained by confocal microscopy corresponding to the adsorption of a fluorescently labeled fibrinogen on surfaces following HHIC: (a) butyl 402, (b) epoxidized butyl 402, (c) epoxidized butyl 402 coated with PEO, (d) PEO on clean silicon wafer, (e) control surface of silane functionalized PEO grafted on glass ($0.01\mu g/cm^2$). Error bars represent the standard deviation of 10 measurements on each of 3 samples.

underway in our laboratory to explore the versatility of this approach.

Resistance of PEO-Functionalized Surfaces to Protein Adsorption. Having demonstrated that HHIC is an effective means of cross-linking PEO to form stable homogeneous films on both silicon wafers and hydrophobic polymer surfaces, the next step was to verify that these films could resist the adsorption of proteins. Fluorescence microscopy was selected as the primary technique to compare the protein adsorption to different surfaces.[58] Fibrinogen was selected as the protein of interest because

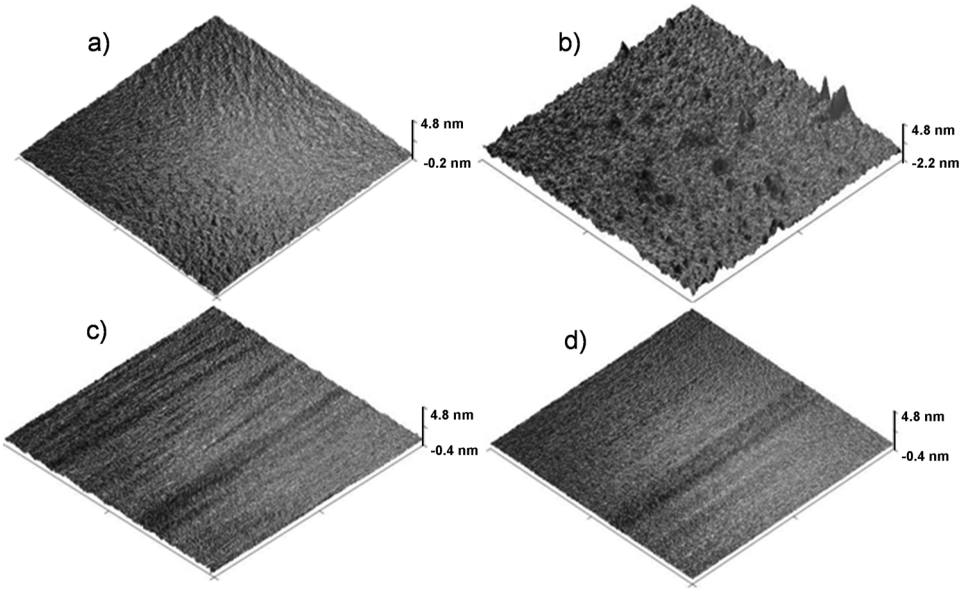

Figure 4. AFM images (topography) before/after protein adsorption: (a) cross-linked butyl rubber before protein adsorption; (b) cross-linked butyl rubber after protein adsorption; (c) cross-linked PEO before protein adsorption; (d) cross-linked PEO after protein adsorption. In each case, the polymers were coated on a silicon wafer. Each image represents a 20 × 20 μm area.

Table 6. XPS Analyses of Cross-Linked PEO- or Butyl 402-Coated Silicon Wafers before or after Protein Adsorption

sample	C 1s	O 1s	N 1s	other
PEO before protein	73.8	26.2		
PEO after protein	72.6	26.5		0.8
butyl before protein	98.5	1.1	0.3	0.1
butyl after protein	55.4	19.9	14.4	10.3

it is a prevalent protein from plasma, involved in the clotting of blood. Fibrinogen has previously received considerable interest because it plays a pivotal role in the process of surface-induced thrombosis.[59] A fluorescent fibrinogen adduct was prepared by its reaction with an activated rhodamine dye as previously reported.[47] In addition, for comparative purposes, a surface in which PEO was grafted chemically was prepared by the reaction of a silane functionalized PEO with clean glass according to the previously reported procedure.[12] Although the fluorescence method does not allow the actual masses of adsorbed protein to be determined, the inclusion of this control sample allows our results to be correlated and compared with a surface for which these values have been previously determined.

To measure the protein adsorption, the butyl, epoxidized butyl, PEO-coated epoxidized butyl, PEO-coated silicon wafer, and chemically grafted PEO surfaces were immersed in a 400 μg/mL solution of fluorescent fibrinogen for 2 h. Following this, the surfaces were washed and confocal fluorescence microscopy was performed at 590 nm. The fluorescence was quantified for at least 10 random regions on each surface and at least 3 surfaces of each type were measured for statistical reasons. As shown in Figure 3, the butyl rubber and epoxidized butyl rubber surfaces exhibited intense fluorescence corresponding to high levels of protein adsorption, a result that can likely be attributed to their high hydrophobicities. In contrast, the PEO coated silicon wafer after 100 s of HHIC exhibited 80-fold lower fluorescence levels. The fluorescence levels of this surface compared favorably with those of the chemically grafted PEO surface. As this particular chemically grafted PEO surface has been measured to adsorb 0.01 μg/cm^2 of protein after 1 h of immersion in a solution of 150 μg/mL,[12] it can be inferred that the values for our cross-linked PEO-coated silicon wafer would be in a similar range under the same experimental conditions. The good performance of the cross-linked PEO films can be attributed to the high surface coverage obtained during the spin coating step, which can be more challenging to obtain in the chemical grafting process as described above. In addition, it confirms that after treatment times of 100 s the nonfouling properties of PEO were retained because the chemical structures of the PEO films were only minimally altered as demonstrated above. For previously reported PEO surfaces generated using plasma treatments, the retention of nonfouling properties have indeed been shown to correlate with the % retention of PEO character.[41,60] Finally, it was found that there was somewhat increased protein adsorption on the PEO coated epoxidized butyl relative to the PEO-coated silicon wafer, likely due to minor inhomogeneities of the coating but this nevertheless corresponded to approximately 10-fold less protein adsorption than on butyl or epoxidized butyl itself. Therefore, the technique can also be effectively applied to unreactive hydrophobic polymer surfaces to achieve significant reductions in protein adsorption. These fluorescence results were also verified qualitatively with AFM where it was found that adsorbed protein and protein aggregates were detected on the cross-linked butyl surface but not on the cross-linked PEO surface (Figure 4). Furthermore, significant amounts of nitrogen were detected by XPS on the butyl surface following protein adsorption, whereas no detectable nitrogen was found on the PEO surface (Table 6).

Knowing that extensive HHIC treatment times alter the structure of the PEO based on the XPS and contact angle results described above, it was also of interest to determine the effects that these changes would have on protein adsorption. Therefore, PEO-coated silicon wafers cross-linked for 100, 400, and 1000 s

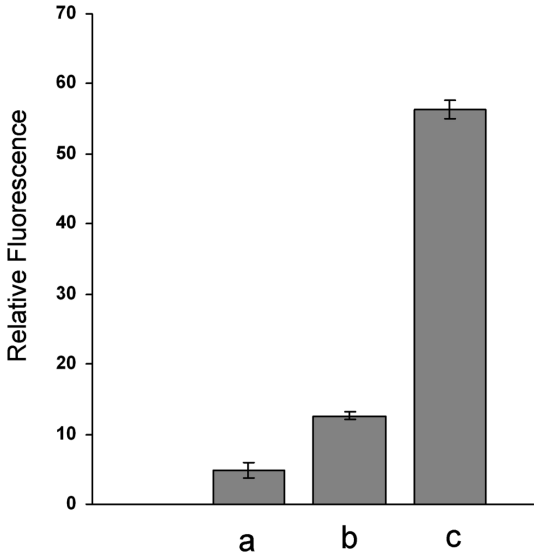

Figure 5. Relative fluorescence values obtained by confocal microscopy corresponding to the adsorption of a fluorescently labeled fibrinogen on PEO coated surfaces following HHIC for (a) 100 s, (b) 400 s, (c) 1000 s. Error bars represent the standard deviation of 10 measurements on each of 3 samples.

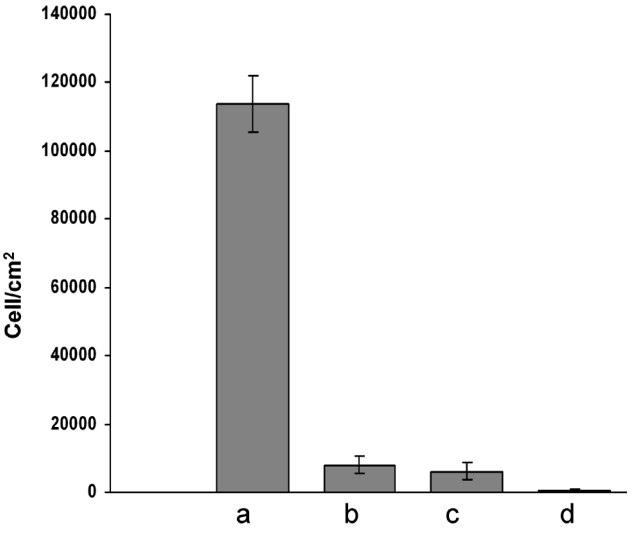

Figure 6. Evaluation of cell growth on surfaces: (a) bulk butyl rubber, (b) butyl + epoxidized butyl + PEO after HHIC, (c) control surface of silane-functionalized PEO grafted on glass, (d) PEO-coated silicon wafer following HHIC. Error bars represent the standard deviation of 10 measurements on each of 3 samples.

were evaluated by the same fluorescence method as above. Indeed the protein adsorption was observed to increase with the treatment time with the 400 and 1000 s samples exhibiting 2.5-fold and 11-fold greater fluorescence, respectively, than the 100 s sample (Figure 5). These results are in agreement with the increasing contact angles with treatment time and were expected because hydrophobicity is known to promote protein adsorption.[61] The decreased PEO chain mobilities resulting from more extensive cross-linking may play a role as the entropy change upon protein binding would be less significant. However, these two effects are difficult to separate in this case.

Resistance of the Surfaces to Cell Adhesion and Growth. Cell adhesion on a substrate is a necessary condition for survival and proliferation of the vast majority of mammalian cells in culture. As cells need to be attached to grow, the evaluation of cell growth on a surface can reflect the ability of this surface to resist cell adhesion. Therefore, the growth of cells on the various surfaces was explored. Each surface was seeded with 10 000 C_2C_{12} mouse fibroblast cells per cm^2 and then the surfaces were incubated for 2 days in culture media. After fixation, the cell nuclei were stained with DAPI, and fluorescence confocal microscopy was used to count the number of cells on the surface. 10 random regions per surface were counted and the surfaces were evaluated in triplicate. As shown in Figure 6, it was found that bulk butyl rubber was a good substrate for cell growth, exhibiting similar cell growth to tissue culture polystyrene (approximately 200 000 cells/cm^2). In contrast, when butyl was coated first with epoxidized butyl as an interfacial layer, followed by PEO and HHIC, the number of cells decreased 10-fold, to a value similar to that observed for the control chemically grafted PEO surface. This reduction in cell adhesion and growth is likely tied to the resistance of these surfaces to protein adsorption as protein adsorption is thought to often be the first step in cell attachment to surfaces.[62]

The PEO cross-linked on the silicon wafer had 24-fold fewer cells than butyl. It is likely that more cells grew on the chemically grafted PEO than on the PEO coated silicon wafer due to the same surface grafting density issue mentioned above. The increased relative cell growth on the PEO coated butyl in comparison with the PEO coated silicon wafer may be because the bulk butyl surface is less smooth and it is therefore more difficult to obtain a fully and uniformly coated surface. Nevertheless, it is significant that it was possible to successfully apply this technique involving both the interfacial epoxidized polymer and HHIC to the bulk polymer surface and achieve a substantial reduction in cell growth.

CONCLUSION

HHIC was used to successfully cross-link PEO on surfaces. Treatment times of 100 s were sufficient to strongly fix the macromolecules on the surface, while at the same time retaining a very high degree of PEO character compared to conventional plasma treatments. Based on fluorescence, AFM, and XPS measurements, this process resulted in resistance to protein adsorption, a result that compared favorably with that of a control chemically grafted PEO surface. Treatment times of 400 s and 1000 s led to the appearance of new functional groups such as O−C═O, C═O, and C−C, as revealed in the high resolution XPS C 1s spectra. These changes in surface composition were accompanied by increased levels of protein adsorption. However, in contrast to conventional plasma methods, which are often accompanied by a loss of oxygen and increase in surface roughness, the C/O ratio and the surface roughness did not change as a result of the HHIC. This can likely be attributed to the selectivity of the method for the cleavage of C−H bonds. It was demonstrated that the method could be successfully applied to hydrophobic non-functional butyl rubber surfaces by using an interfacial layer of epoxidized polymer. Furthermore, the resistance of the PEO functionalized surfaces to protein adsorption also translated into resistance of the surfaces to the growth of cells. Overall, these results suggest that HHIC is a promising method for imparting non-fouling properties to a diverse array of unreactive hydrophilic and hydrophobic surfaces containing C−H bonds

and that it may also be possible to apply the method to polymers containing functional groups other than those found in PEO.

■ ASSOCIATED CONTENT

Supporting Information. Details concerning the HHIC process, effects of treatment time on film roughness, AFM of a PEO film demonstrating the measurement of film thickness, high-resolution XPS spectra for PEO films following different treatment times, chemical scheme illustrating the formation of cyclic ethers, confocal microscopy images of surfaces following protein adsorption, and fluorescence microscopy images of cell growth on surfaces. This material is available free of charge via the Internet at http://pubs.acs.org.

■ AUTHOR INFORMATION

Corresponding Author
*E-mail: egillie@uwo.ca.

■ ACKNOWLEDGMENT

We thank LANXESS Inc. for funding of this work and for providing samples of butyl rubber. The Ontario Centres of Excellence and the Natural Sciences and Engineering Research Council of Canada are also thanked for funding.

■ REFERENCES

(1) Krishnan, S.; Weinman, C. J.; Ober, C. K. *J. Mater. Chem.* **2008**, *18*, 3405–3413.
(2) Roach, P.; Eglin, D.; Rohde, K.; Perry, C. C. *J. Mater. Sci. Mater. Med.* **2007**, *18*, 1263–1277.
(3) Harris, M. J. *Poly(ethylene glycol) Chemistry: Biotechnical and Biomedical Applications*; Plenum Press: New York, 1992.
(4) Leckband, D.; Sheth, S.; Halperin, A. *J. Biomater. Sci. Polym. Ed.* **1999**, *10*, 1125–1147.
(5) Jeon, S. I.; Andrade, J. D. *J. Colloid Interface Sci.* **1991**, *142*, 159–166.
(6) Halperin, A. *Langmuir* **1999**, *15*, 2525–2533.
(7) Chan, Y. H. M.; Schweiss, R.; Werner, C.; Grunze, M. *Langmuir* **2003**, *19*, 7380–7385.
(8) Herrwerth, S.; Eck, W.; Reinhardt, S.; Grunze, M. *J. Am. Chem. Soc.* **2003**, *125*, 9359–9366.
(9) Kreuzer, H. J.; Wang, R. L. C.; Grunze, M. *J. Am. Chem. Soc.* **2003**, *125*, 8384–8389.
(10) Ryle, A. P. *Nature* **1965**, *206*, 1256.
(11) McPherson, T.; Kidane, A.; Szleifer, I.; Park, K. *Langmuir* **1998**, *14*, 176–186.
(12) Jo, S.; Park, K. *Biomaterials* **2000**, *21*, 605–616.
(13) Murthy, R.; Cox, C. D.; Hahn, M. S.; Grunlan, M. A. *Biomacromolecules* **2007**, *8*, 3244–3252.
(14) Yang, Z.; Galloway, J. A.; Yu, H. *Langmuir* **1999**, *15*, 8405–8411.
(15) Dong, B.; Jiang, H.; Manolache, S.; Wong, A. C. L.; Denes, F. S. *Langmuir* **2007**, *23*, 7306–7313.
(16) Sofia, S. J.; Premnath, V.; Merril, E. *Macromolecules* **1998**, *31*, 5059–5070.
(17) Hoffmann, J.; Groll, J.; Heuts, J.; Rong, H.; Klee, D.; Ziemer, G.; Moeller, M.; Wendel, H. P. *J. Biomater. Sci., Polym. Ed.* **2006**, *17*, 985–996.
(18) Alcantar, N. A.; Aydil, E. S.; Israelachvili, J. N. *J. Biomed. Mater. Res.* **2000**, *51*, 343–351.
(19) Gong, X.; Dai, L.; Griesser, H. J.; Mau, A. W. H. *J. Polym. Sci., Part B: Polym. Phys.* **2000**, *38*, 2323–2332.
(20) Norde, W.; Gage, D. *Langmuir* **2004**, *20*, 4162–4167.
(21) Unsworth, L. D.; Sheardown, H.; Brash, J. L. *Langmuir* **2005**, *21*, 1036–1041.
(22) Michel, R.; Pasche, S.; Textor, M.; Castner, D. G. *Langmuir* **2005**, *21*, 12327–12332.
(23) Unsworth, L. D.; Sheardown, H.; Brash, J. L. *Langmuir* **2008**, *24*, 1924–1929.
(24) Lee, J. H.; Kopecek, J.; Andrade, J. D. *J. Biomed. Mater. Res.* **1989**, *23*, 351–368.
(25) Liu, V. A.; Jastromb, W. E.; Bhatia, S. N. *J. Biomed. Mater. Res.* **2002**, *60*, 126–134.
(26) Ji, J.; Feng, L.; Shen, J. *Langmuir* **2003**, *19*, 2643–2648.
(27) Prime, K. L.; Whitesides, G. M. *J. Am. Chem. Soc.* **1993**, *115*, 10714–10721.
(28) Benhabbour, S. R.; Sheardown, H.; Adronov, A. *Macromolecules* **2008**, *41*, 4817–4823.
(29) Ma, H. W.; Hyun, J. H.; Stiller, P.; Chilkoti, A. *Adv. Mater.* **2004**, *16*, 338–341.
(30) Hucknall, A.; Rangarajan, S.; Chilkoti, A. *Adv. Mater.* **2009**, *21*, 2441–2446.
(31) Knoll, D.; Hermans, J. *J. Biol. Chem.* **1983**, *258*, 5710–5715.
(32) Zhu, X. Y.; Jun, Y.; Staarup, D. R.; Major, R. C.; Danielson, S.; Boiadjiev, V.; Gladfelter, W. L.; Bunker, B. C.; Guo, A. *Langmuir* **2001**, *17*, 7798–7803.
(33) Sheu, M. S.; Hoffman, A. S.; Feijen, J. *J. Adhes. Sci. Technol.* **1992**, *6*, 995–1009.
(34) Yen, C.; He, H. Y.; Fei, Z. Z.; Zhang, X. L.; Lee, L. J.; Ho, W. S. W. *Int. J. Polym. Mater.* **2010**, *59*, 923–942.
(35) D'Sa, R. A.; Meenan, B. J. *Langmuir* **2010**, *26*, 1894–1903.
(36) Sofia, S. J.; Merrill, E. W. *J. Biomed. Mater. Res.* **1998**, *40*, 153–163.
(37) Shen, M.; Wagner, M. S.; Castner, D. G.; Ratner, B. D.; Horbett, T. A. *Langmuir* **2003**, *19*, 1692–1699.
(38) Lopez, G. P.; Ratner, B. D. *Plasmas Polym.* **1995**, *1*, 127–151.
(39) Bretagnol, F.; Ceriotti, L.; Lejeune, M.; Papadopoulou-Bouraoui, A.; Hasiwa, M.; Gilliland, D.; Ceccone, G.; Colpo, P.; Rossi, F. *Plasma Processes Polym.* **2006**, *3*, 30–38.
(40) Sardella, E.; Detomaso, L.; Gristina, R.; Senesi, G. S.; Agheli, H.; Sutherland, D. S.; d'Agostino, R.; Favia, P. *Plasma Processes Polym.* **2008**, *5*, 540–551.
(41) Sardella, E.; Gristina, R.; Senesi, G. S.; d'Agostino, R.; Favia, P. *Plasma Processes Polym.* **2004**, *1*, 63–72.
(42) Padron-Wells, G.; Jarvis, B. C.; Jindal, A. K.; Goeckner, M. J. *Colloids Surf., B* **2009**, *68*, 163–170.
(43) Chu, L. Q.; Knoll, W.; Forch, R. *Chem. Mater.* **2006**, *18*, 4840–4844.
(44) Palumbo, F.; Favia, P.; Vulpio, M.; d'Agostino, R. *Plasmas Polym.* **2001**, *6*, 163–174.
(45) Zheng, Z.; Xu, X. D.; X.L., F.; Lau, W. M.; Kwok, R. W. M. *J. Am. Chem. Soc.* **2004**, *126*, 12336–12342.
(46) Liu, Y.; Yang, D. Q.; Nie, H.-Y.; Lau, W. M.; Yang, J. *J. Chem. Phys.* **2011**, *134*, 074704/1–8.
(47) Bonduelle, C. V.; Gillies, E. R. *Macromolecules* **2010**, *43*, 9230–9233.
(48) Lopez, G. P.; Ratner, B. D.; Tidwell, C. D.; Haycox, C. L.; Rapoza, R. J.; Horbett, T. A. *J. Biomed. Mater. Res.* **1992**, *26*, 415–439.
(49) Currie, E. P. K.; van der Gucht, J.; Borisov, O. V.; Cohen Stuart, M. A. *Pure Appl. Chem.* **1999**, *71*, 1227–1241.
(50) Lee, J. H.; Lee, H. B.; Andrade, J. D. *Prog. Polym. Sci.* **1995**, *20*, 1043–1079.
(51) Andrade, J. D.; Hlady, V.; Jeon, S. I. *Adv. Chem. Ser.* **1996**, *248*, 51–59.
(52) Jeon, S. I.; Lee, J. H.; Andrade, J. D.; De Gennes, P. G. *J. Colloid Interface Sci.* **1991**, *142*, 149–158.
(53) Favia, P.; Sardella, E.; Gristina, R.; d'Agostino, R. *Surf. Coat. Technol.* **2001**, *169-170*, 707–711.
(54) Puskas, J. E.; Chen, Y. *Biomacromolecules* **2004**, *5*, 1141–1154.
(55) Puskas, J. E.; Chen, Y.; Dahman, Y.; Padavan, D. *J. Polym. Sci., Part A: Polym. Chem.* **2004**, *42*, 3091–3109.
(56) Pinchuk, L.; Wilson, G. J.; Barry, J. J.; Schoephoersterd, R. T.; Parele, J.-M.; Kennedy, J. P. *Biomaterials* **2008**, *29*, 448–460.

(57) Ocando, C.; Tercjak, A.; Serrano, E.; Ramos, J. A.; Corona-Galvan, S.; Parellada, M. D.; Fernandez-Berridi, M. J.; Mondragon, I. *Polym. Int.* **2008**, *57*, 1333–1342.
(58) Model, M. A.; Healy, K. E. *J. Biomed. Mater. Res.* **2000**, *50*, 90–96.
(59) Horbett, T. A. *Cardiovasc. Pathol.* **1993**, *2*, S137.
(60) Morra, M. In *Water in Biomaterials Surface Science*; Morra, M., Ed.; John Wiley and Sons: NewYork, 2001, p 307−332.
(61) Wang, Y. X.; Robertson, J. L.; Spillman, W. B.; Claus, R. O. *Pharm. Res.* **2004**, *21*, 1362–1373.
(62) Shard, A. G.; Tomlins, P. E. *Regenerative Med.* **2006**, *1*, 789–800.